Partitioning of bacterial communities between travertine depositional facies at Mammoth Hot Springs, Yellowstone National Park, U.S.A.[1]

Bruce W. Fouke, George T. Bonheyo, Beth Sanzenbacher, and Jorge Frias-Lopez

Abstract: A culture-independent molecular survey indicates that the composition of bacterial communities is distinctly partitioned between travertine depositional facies in the surface drainage system of Spring AT-1 at Angel Terrace, Mammoth Hot Springs, Yellowstone National Park. PCR (polymerase chain reaction) amplification and sequencing of 16S rRNA genes with universally conserved bacterial primers has identified over 553 unique partial and 104 complete gene sequences (derived from more than 14 000 clones), affiliated with 221 unique species that represent 21 bacterial divisions. These sequences exhibited < 12% similarity in bacterial community composition between each of the travertine depositional facies. This implies that relatively little downstream bacterial transport and colonization took place despite the rapid and continuous flow of spring water from the high-temperature to low-temperature facies. These results suggest that travertine depositional facies, which are independently determined by the physical and chemical conditions of the hot spring drainage system, effectively predict bacterial community composition as well as the morphology and chemistry of travertine precipitation.

Résumé : Un relevé moléculaire, indépendant des cultures, indique que la composition des communautés bactériennes est répartie de façon distincte entre les faciès de déposition de travertin dans le système de drainage de surface de la source AT-1 à Angel Terrace, Mammoth Hot Springs, du parc national Yellowstone. Une amplification PCR et le séquençage des gènes 16S rARN avec des amorces bactériennes universellement conservées a permis l'identification de plus de 553 séquences partielles uniques et 104 séquences complètes de gènes (dérivées de plus de 14 000 clones) affiliées à 221 espèces uniques qui représentent 21 divisions bactériennes. Dans la composition de la communauté bactérienne, les séquences montrent moins de 12 % de similitude entre chacun des faciès de déposition du travertin. Cela implique qu'il s'effectue peu de transport bactérien vers l'aval et qu'une colonisation a lieu malgré l'écoulement rapide et continuel des eaux de source du faciès de haute température vers le faciès de basse température. Ces résultats suggèrent que les faciès de déposition du travertin, qui sont définis de façon indépendante par les conditions physiques et chimiques du système de drainage des sources thermales, prédisent effectivement la composition de la communauté bactérienne et la morphologie et la chimie de la précipitation du travertin.

[Traduit par la Rédaction]

Introduction

A fundamental scientific endeavor unique to the geosciences over the last 170 years has been the reconstruction of ancient earth surface environmental conditions from the analysis of ancient sedimentary rocks (Blatt et al. 1980; Reading 1996; Boggs 2002). To accomplish this, workers have studied the interaction of physical, chemical, and biological processes in modern-day sedimentary environments that deposit analogous sedimentary rocks. This work has resulted in the development of depositional *facies* models that correlate (1) the depth, velocity, temperature, and chemistry of water in the environment; (2) the grain size, sorting, mineralogy, structure, and geometry of sediments being deposited; and (3) the animal and plant communities living in each community (e.g., Walker and James 1992).

Sedimentary facies models provide an essential process-oriented conceptual tool to systematically break down larger complex depositional environments into smaller sub-environments, each of which are linked along continuous hydrologic environmental gradients. Facies models are independent of the relative size and specific location of the environment being studied, and thus have nearly universal applicability in settings that range from terrestrial glaciers to marine coral reefs (Blatt et al. 1980; Reading 1996; Boggs 2002). Of equal importance, facies models create sys-

Received 5 February 2003. Accepted 11 June 2003. Published on the NRC Research Press Web site at http://cjes.nrc.ca on 25 November 2003.

Paper handled by Associate Editor B. Chatterton.

B.W. Fouke,[2] G.T. Bonheyo, B. Sanzenbacher, and J. Frias-Lopez. Department of Geology, University of Illinois Urbana-Champaign, Urbana, IL 61801, U.S.A.

[1]This article is one of a selection of papers published in this Special Issue on *Sedimentology of hot spring systems*.

[2]Corresponding author (e-mail: fouke@uiuc.edu).

 doi: 10.1139/E03-067

tematic spatial and temporal frameworks within which detailed analyses of geochemistry and macroorganisms (plants and animals) can be holistically linked to system-scale environmental processes (Wilson 1975; Flügel 1982; Walker and James 1992). However, with the notable exception of stromatolites (Walker and James 1992), depositional facies models have lacked detailed evaluation of the pivotal role that may be played by microorganisms during sediment deposition and associated water–rock reactions. This is presumably because no previous study of modern sedimentary facies models has included culture-independent molecular analyses (see summary in Pace 1997) of the bacteria inhabiting each facies.

The purpose of the present study is to complete the first comprehensive survey of bacterial 16S rRNA gene sequences in the context of the depositional facies that the bacteria inhabit. The study site for this analysis is the surface drainage system of the terrestrial carbonate hot spring called Spring AT-1 on Angel Terrace in the Mammoth Hot Springs complex of Yellowstone National Park (Fouke et al. 2000). This location was chosen because the physical, chemical, and biological conditions of the spring water change drastically as it flows away from the vent, and these conditions are associated with the precipitation of carbonate mineral deposits called *travertine* (sensu strictu Pentecost and Viles 1994; Ford and Pedley 1996). These environmental changes create a systematic series of five travertine depositional facies along the Spring AT-1 drainage system, each of which have previously been defined by their aqueous chemistry and travertine morphology and chemistry (Fouke et al. 2000). Results are presented in the present study that indicate that the composition of the bacterial community inhabiting each travertine facies is more than 87% unique from the next directly adjoining down flow facies. This suggests that the travertine facies model is an accurate predictive tool for bacterial community composition in addition to the morphology and chemistry of travertine deposition.

Geological setting

Geothermal groundwater erupts at a temperature of 73 °C from subsurface conduits at Spring AT-1 on Angel Terrace in the Mammoth Hot Springs complex (Fig. 1), creating a series of terraced travertine deposits (Allen and Day 1935; Bargar 1978; Fig. 2). As the Spring AT-1 groundwater cools, degasses, and flows along surface drainage channels, travertine composed of aragonite and calcite ($CaCO_3$) is precipitated at rates as high as 5 mm/day (Friedman 1970; Pentecost 1990; Fouke et al. 2000). The travertine depositional facies described from the Spring AT-1 drainage system in Fouke et al. (2000) is briefly summarized in the following.

Angel Terrace Spring AT-1 is composed of a series of shallow-water environments extending from the spring vent to the distal parts of the system. These aqueous environments and their associated travertine deposits are divisible into five depositional facies: (1) vent facies, (2) apron and channel facies, (3) pond facies, (4) proximal-slope facies, and (5) distal-slope facies (Fig. 2). The boundaries of the facies are based on systematic changes in travertine crystal morphology and chemistry and associated changes in water chemistry. The composition and relative sequence of the facies has been observed in other springs and is consistently re-established

Fig. 1. Location of Spring AT-1 at Angel Terrace in the Mammoth Hot Springs complex of Yellowstone National Park. Shading depicts the surface area covered by the Spring AT-1 waters as the flow away from the vent (shown by a ●).

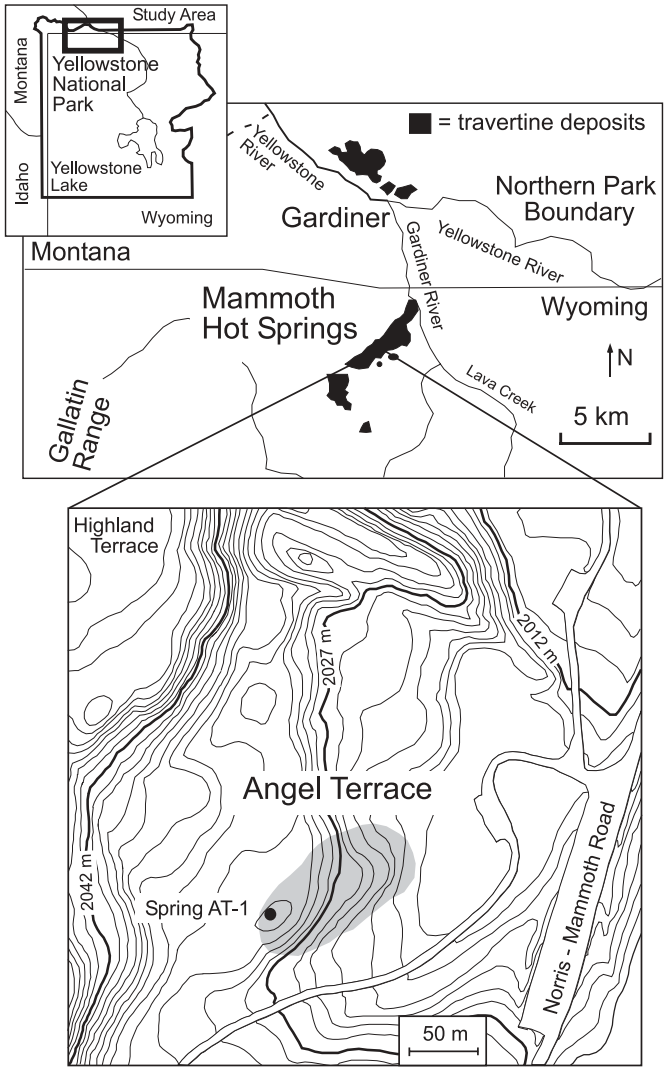

as the springs shift their position due to changes in spring water flow velocity and the opening of new vents (Fouke et al. 2000; Fouke 2001). Travertine precipitated in each of the Spring AT-1 facies exhibits distinct growth forms and chemistries, which are accompanied by a general transition in mineralogy from aragonite in the high-temparture waters to calcite in the low-temperature waters (Fig. 2). The water in the drainage system ranges from depths of approximately 1 to 30 cm and flows over substrates composed of actively precipitating travertine and living microbial mats. Water temperature decreases from 73 to 18 °C. Vent water temperatures are invariant throughout the year, while the distal-slope waters reach their minimum temperatures in the winter (Fouke et al. 2000; Fig. 2). The inconsistent drops in water temperature observed along the drainage system (Fig. 2) are caused by lateral diversions in flow and the variability in water depth between each facies. Spring water pH increases from 6.2 at the vent to 8.7 in the distal-slope (Fig. 2). This is accompanied by large magnitude changes in the chemistry

Fig. 2. Field photograph (A) and schematic cross-section (B) of Spring AT-1 at Angel Terrace, indicating travertine depositional facies distributions, spring water temperature and pH, travertine mineralogy, flow directions, and rates of travertine precipitation. Note the large well-developed terracette pool in the center of the photograph, which forms the characteristic terraced travertine geomorphology of Angel Terrace and the Mammoth Hot Spring complex.

A

B

Facies	Vent	Apron and Channel	Pond	Proximal Slope	Distal Slope
Temp (°C)	69.3 - 72.6	65.0 - 71.2	34.6 - 58.9	38.1 - 55.4	18.0 - 37.9
pH	6.2 - 6.7	6.5 - 7.0	7.4 - 8.6	7.7 - 8.1	8.2 - 8.7
Minerals	aragonite	aragonite	aragonite and calcite	aragonite and calcite	calcite

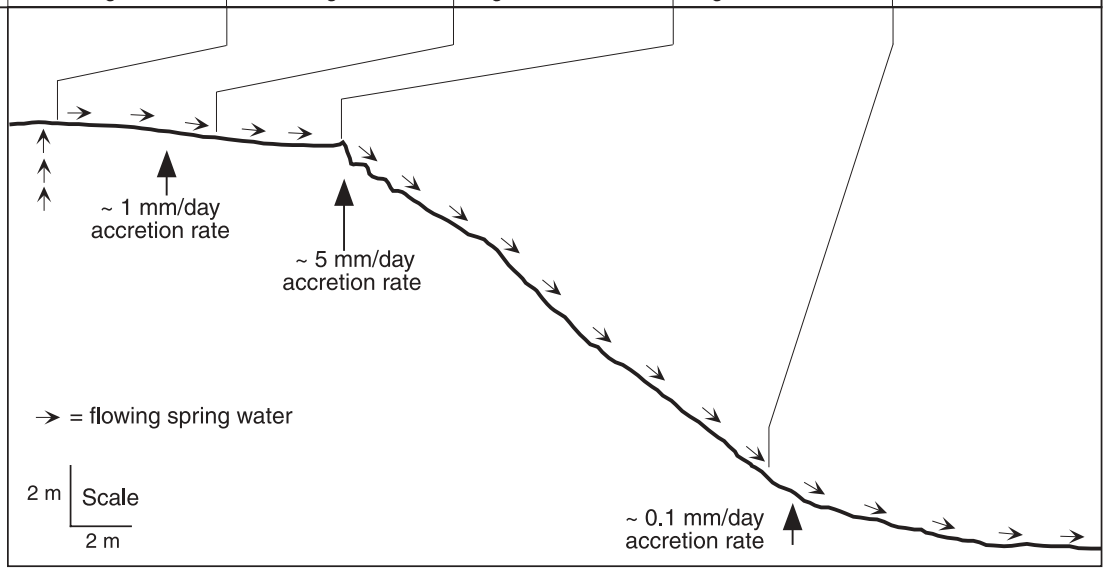

Fig. 3. Field photographs of the travertine depositional facies composing the Spring AT-1 drainage system at Angel Terrace. (A) Overview of the vent facies and apron and channel facies showing trees that have been inundated by travertine deposition. (B) View of the vent within the vent facies, where spring water is 73 °C with water depths of 30 cm. (C) Gradational contact of the vent facies and apron and channel facies, where water depths shallow from 30 cm to 1 cm. (D) Abrupt contact between the apron and channel facies and the pond facies. (E) Enlargement of the sharp facies contact shown in D. (F) Microterracettes forming at the sharp contact between the pond facies (pooled water lapping against the lip of the terracette at the top of the photograph) and the nearly vertical proximal-slope facies. (G) Small pools and microterracettes composing the proximal-slope facies. (H) Broad and shallow microterracette pools composing the distal-slope facies.

of the spring water (total dissolved inorganic carbon, $\delta^{13}C$, $\delta^{18}O$, $^{87}Sr/^{86}Sr$, dissolved sulfate, $\delta^{34}S$) and travertine ($\delta^{13}C$, $\delta^{18}O$, $^{87}Sr/^{86}Sr$, $\delta^{34}S$; Fouke et al. 2000).

The vent facies (5–30 cm water depth) contains mounded travertine composed of aragonite needle botryoids (Figs. 3A–3C, 4A, 4B). The vent facies transitions into the apron and channel facies (≤5 cm water depth), which is floored by hollow travertine tubes composed of aragonite needle botryoids that encrust filamentous thermophilic bacteria (Figs. 3A–3D, 4C, 4D). The transition into the pond facies is an abrupt contact, with the pooled pond waters reaching depths of 30 cm. Travertine in the pond facies forms large step-like morphologies called *terracettes* that include aragonite needle shrubs at higher temperatures and ridged networks of calcite and aragonite at lower temperatures (Farmer 2000). In addition, calcite "ice sheets," calcified bubbles, and aggregates of aragonite needles ("fuzzy dumbbells") precipitate at the air–water interface and settle to pond floors (Figs. 3D, 3E, 4D, 4E; Fouke et al. 2000). An abrupt facies transition is exhibited at the margins (or lips) of the pond pools. The proximal-slope facies (≤3 cm water depth), which is composed of arcuate aragonite needle clusters that create small fluted microterracettes on the steep slope face (Figs. 3F, 3G, 4F, 4G). Finally, a gradual transition takes place into the distal-slope facies (≤2 cm water depth), where travertine forms broad low-relief microterracettes that are composed entirely of calcite spherules and "feather" calcite crystals (Figs. 3H, 4H).

The aqueous chemistry of the hot spring drainage system is strongly influenced by CO_2 degassing, as indicated by Rayleigh-type fractionation calculations of spring water $\delta^{13}C$ versus dissolved inorganic carbon concentrations (Fouke et al. 2000). However, while the physical factors of temperature decrease and degassing are significant in helping to drive the rapid precipitation of travertine, strong bacterial influences on travertine crystal form and isotope composition have also been observed throughout the Spring AT-1 drainage system. One important example is aragonite crystals that encrust and thus preserve the shape of filamentous bacteria as hollow travertine "streamers" in the vent, as well as apron and channel facies (Farmer and Des Marais 1994; Fouke et al. 2000; Farmer 2000). A chemical expression of biological influence is the disequilibrium fractionation observed in the $\delta^{13}C$, $\delta^{18}O$, and $\delta^{34}S$ composition of the travertine, which can be detected only after the fractionation effects of CO_2 degassing and temperature drop have been quantitatively subtracted (Fouke et al. 2000).

Materials and methods

Field sampling of spring water, microbial mats, and fresh travertine precipitated on the floor of the Spring AT-1 drainage system was completed during daylight hours in January 1999, as well as January and May 2000. Fifty samples were collected for analysis over this time period from the five travertine depositional facies (Fig. 2). Use of the travertine facies model permitted sampling in equivalent spring environments in 2000 after the drainage system had shifted laterally from its original position in 1999 due to temporal changes in the flow velocity and travertine precipitation of hot groundwater emerging from the Spring AT-1 vent.

Sample collection

Spring water was sampled by collecting 2 L from each facies in acid-cleaned 1 L Nalgene HDPE bottles. The water was hand-pumped through a sterile 0.45 μm filter-loaded cup (Pall/Gelman). All filters were then immediately frozen at –20 °C, transported to Illinois on dry ice and stored at –40 to –80 °C. Travertine was collected by removing a 2 cm^2 portion of the uppermost 0.25–1 cm of the floor of the drainage flow path with a cleaned spatula and placing the sample in a sterile disposable 50 mL polypropylene centrifuge tube. Portions of the microbial mats growing on the travertine substrates were also physically peeled off and collected using forceps. Microbial mat samples were immersed in 80% ethanol in sterile 15 mL polypropylene centrifuge tubes. Travertine substrate samples were crushed and homogenized in sterile 15 mL polypropylene centrifuge tubes with sterile blades, creating a slurry of ethanol, microbial mats, loose microorganisms, and travertine crystals.

DNA extraction

Several methods of DNA extraction were used with each sample to increase the likelihood that no microorganism would escape detection. Filters were sectioned using flame sterilized scissors and forceps and placed in sterile disposable 50 mL polypropylene centrifuge tubes with 3 mL of sterile ultra pure water. Cells were then washed off the filter during three minutes of vigorous agitation on a vortex and stored frozen at –80 °C.

Bead beating (Hugenholtz et al. 1998), freeze–thaw cycling, and chemical lysis protocols (Sambrook et al. 1989) were used to extract community genomic DNA from the cells collected on the filters, the crushed travertine slurries, and the microbial mat samples. For bead beating, 300 μL of sample was added to a 2 mL screw-capped microcentrifuge tube containing 600 μL of sterile ultra pure water and 800 μL of 0.1 mm zirconia–silica beads (BioSpec Products, Bartlesville, Okla.). The beads were cleaned and sterilized beforehand with a series of HCl acid and bleach washes. The tube was then filled to capacity with sterile ultra pure water and shaken on a reciprocating Mini-BeadBeater-8 (BioSpec Products, Bartlesville, Okla.) for 2.5 min at the homogenize (highest)

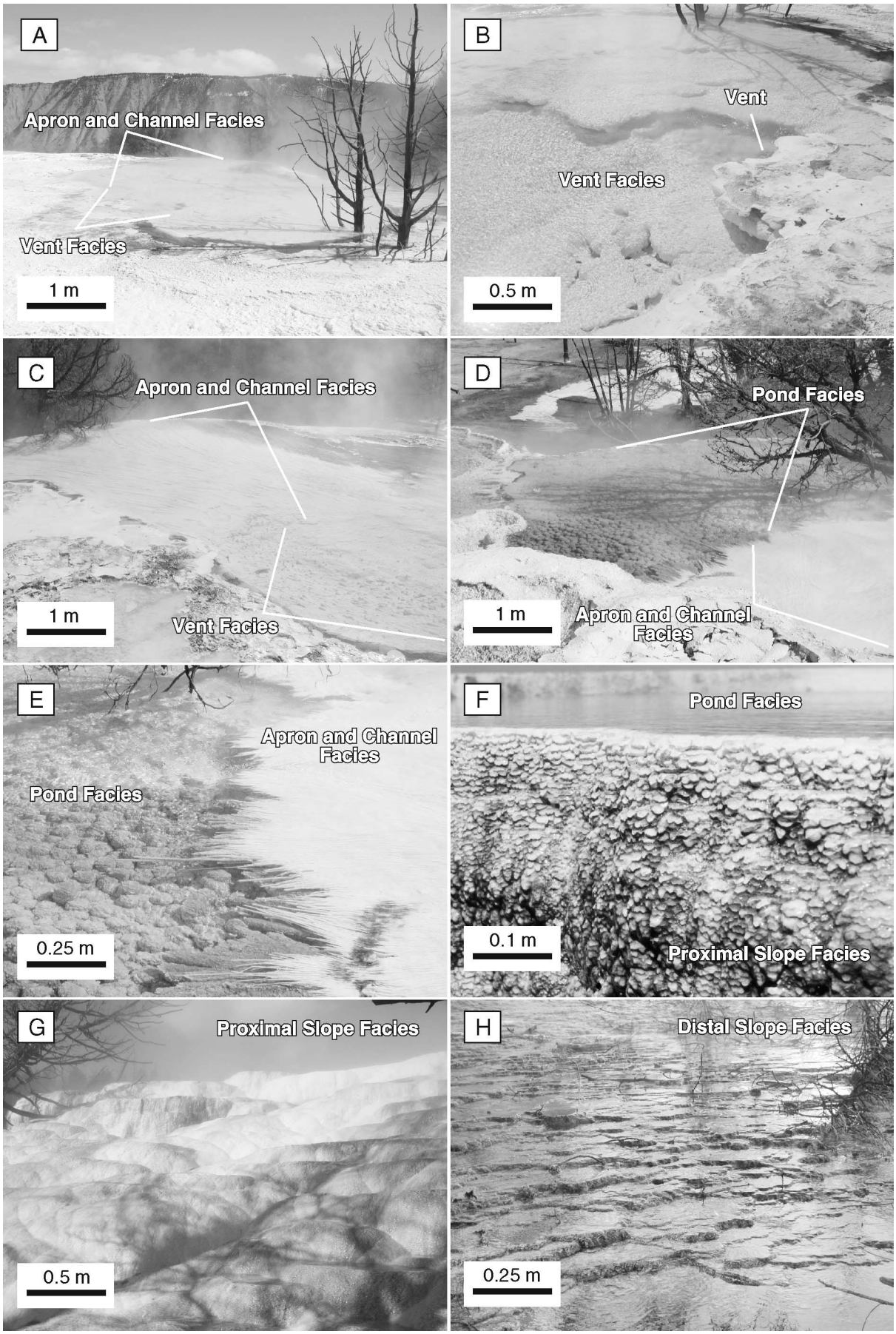

Fig. 4. Close-up field photographs of the travertine depositional facies comprising the Spring AT-1 drainage system at Angel Terrace. (A) The vent within the vent facies (white box shows the sample collection position of the photograph in B). (B) Handsample of mounded travertine deposits from the vent facies. (C) Floor of the apron and channel facies composed of hollow sinuous aragonitic travertine tubes viewed through < 2 cm of swiftly flowing spring water. (D) Enlargement of the sharp contact between the apron and channel facies and the pond facies, showing long filamentous strands of *Aquificales* pBB that project out into the pond and are being encrusted by aragonite needles to form slender hollow tubes of travertine. (E) Floor of the pond facies composed of spherical clusters of shrub-like aragonite travertine. (F) View looking directly down on the sharp lip of the pond, illustrating the abrupt transition from the aragonite shrubs on the floor of the pond facies to the aragonitic microterracettes covering the face of the proximal-slope facies. (G) Aragonite microterracettes forming in the central portion of the proximal-slope facies submerged under < 1 cm of swiftly flowing spring water. (H) A broad and shallow (<1 cm water depth) travertine microterracette composed of calcite in the distal-slope facies.

speed setting. This protocol has been optimized using several samples, as well as *E. coli* positive controls. For the freeze–thaw procedure, samples were added to sterile 2 mL O-ring screw-capped microcentrifuge tubes containing 1 mL of sterile ultra pure water. The tubes were frozen at –80 °C and rapidly thawed by plunging the tubes into a 65 °C water bath. The freeze–thaw cycle was repeated three times, with the tubes vigorously agitated on a vortex for ~ 1 min after each thaw cycle. In some instances, samples were treated with an alkaline lysis step using NaOH (0.13 M final (1 M = 2 mol/L)), sodium dodecyl sulfate (SDS, 0.3%), and incubation at 25 to 100 °C for 2 min (Sambrook et al. 1989).

For both the bead beating and freeze–thaw techniques, a 400 μL aliquot of the lysate was used for additional DNA precipitation using two volumes absolute ethanol, followed by a series of washing steps using 70% EtOH (Sambrook et al. 1989). The ethanol precipitated lysates, untreated lysates, and untreated samples were used in subsequent PCRs (polymerase chain reactions). Each protocol routinely included 300 μL of the sterile ultra pure water as both a negative control and contamination screen, and 50 μL of an overnight Luria broth *E. coli* culture as a positive control. The control preparations were included with their simultaneously prepared environmental samples each time a PCR reaction was performed. In no case were nucleic acids detected in the negative controls.

PCR Amplification

Total environmental chromosomal DNA was used as template for PCR amplification of 16S rRNA genes using a Mastercycler Gradient thermocycler (Eppendorf, Westbury, N.Y.) and universal 16S rRNA primers for Bacteria. Primers used in the PCRs were obtained from Operon Technologies, Inc. (Alemeda, Calif.). B. Paster (personal communication, 1998) provided the sequence of each primer: forward primer: 28F (5′-GAGTTTGATYMTGGCTC); reverse primer: 1492R (5′-GYTACCTTGTTACGACTT). Reaction mixtures included a final concentration of: 1X TaqMaster buffer (Eppendorf), 1x TaqM enhancer (Eppendorf), 0.2 mM each dNTP (Gibco/BRL, Rockville, Md.), 200 ng each of forward and reverse primers, 5–30 μL of the sample preparation, and water to bring the total volume to 100 μL. Reactions were layered beneath 50 μL of mineral oil (Sigma, St. Louis, Mo.). An initial denaturation – hot start of 5 min at 95 °C was followed by the addition of 0.5 μL (~2 U) of MasterTaq polymerase (Eppendorf) or *Taq* DNA polymerase (Gibco/BRL, Rockville, Md.). The hot start was followed by 30 cycles of the following incubation pattern: 94 °C for 1 min, 55 °C for 1 min, and 72 °C for 2 min. A final soak at 72 °C for 5 min concluded the reaction. All PCRs were mixed and run in an enclosed PCR work station to prevent contamination.

Cloning and sequencing

PCR products were purified by electrophoresis through a 1.0% low-melting agarose gel (SeaPlaque GTG; BioWhittaker Molecular Applications, Rockland, Maine), stained with ethidium bromide and visualized on a UV (ultraviolet) trans-illuminator. The ~1500 bp heterologous 16S rRNA gene product was excised from the gel, and the DNA was purified from the gel slice using the Wizard PCR Prep kit (Promega, Madison, Wis.). The gel-purified PCR product was cloned into the pGEM-T Easy vector (Promega) and transformed into calcium chloride competent DH5αMCR *E. coli* cells (Gibco/BRL) using standard techniques (Sambrook et al. 1989). Clone libraries were created by patching transformants in 6 × 8 grids on standard Luria broth agar (100 μg/mL of Ampicilin and 40 μg/mL X-Gal) petri dishes. The clone libraries were then screened to verify the presence of the appropriate sized insert to identify unique clones for sequencing. Petri dish libraries were inoculated using a 48-pin replicator (Midwest Scientific, St. Louis, Mo.) into 96-well culture blocks (2 mL well capacity) containing Luria broth (15% glycerol and 100 μg/mL of Ampicilin). Culture blocks were sealed with AirPore tape (Qiagen, Valencia, Calif.) and shaken overnight at 37 °C. On the following day, 3 μL from each well was transferred to a 96-well flex-plate (GeneMate, Kaysville, Utah) containing 27 μL of PCR mixture (0.2 mM dNTP (Gibco/BRL, Rockville, Md.), 1x PCR Buffer (Gibco/BRL), 0.8U Taq (Gibco/BRL), 1.5 mM $MgCl_2$, and 200 ng each of T7(-26) forward and M 13(-48) reverse primers). The culture block was then sealed with plastic tape (Qiagen) and the remaining culture was frozen at –80 °C. The flex-plates were sealed with tape (Qiagen) and a 30-cycle PCR amplification was carried out as previously described. Because the forward and reverse primer sequences are located on the pGEM-T vector flanking the cloning site, only insert DNA is amplified. After amplification, 8 μL from each flex-plate well was transferred to a new well of a 96-well microtiter plate containing 32 μL of restriction digest mixture consisting of the 4-base recognition site enzymes *Msp*I and *Hin*P1 I in 1x NEB Buffer 2 (New England Biolabs, Beverly, Mass.). The digest products were then separated by electrophoresis on a 3.0% agarose gel (MetaPhor; BioWhittaker Molecular Applications, Rockland, Maine) stained with ethidium bromide, and the RFLP (restriction fragment length polymorhism) patterns used to identify unique clones to be submitted for sequence analysis. Three to five samples with seemingly identical RFLP patterns

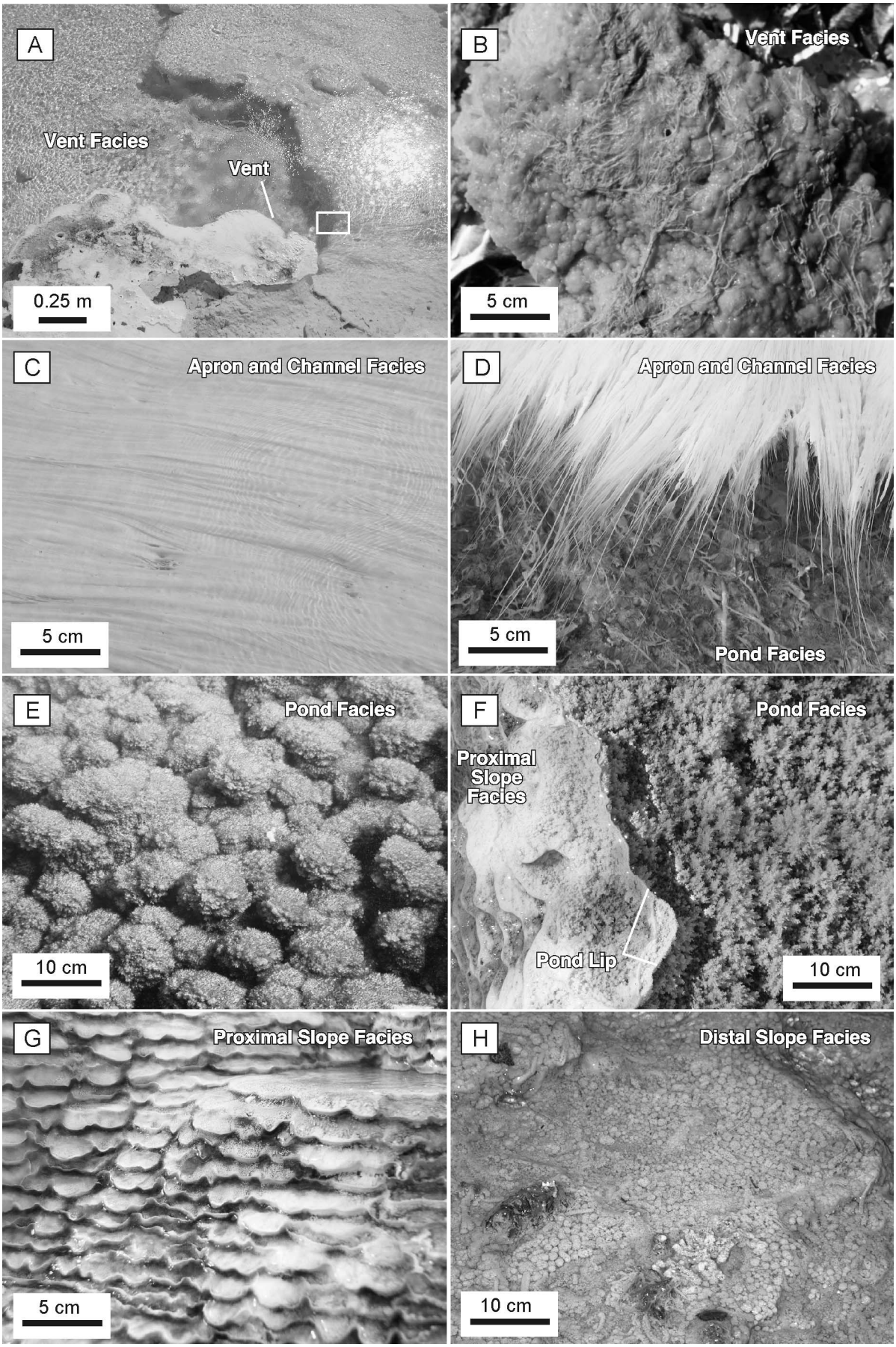

Table 1. 16S rRNA gene sequencing results for bacteria inhabiting the Spring AT-1 vent facies.

ID%	Bp	Access.	Best match organism	Division facies	V	AC	P	PS	DS
96–98	1484	AF445739	Uncultured Aquificales pBB	Aquificales	45	2	17	34	1
97–99	1483	AF445734	Unidentified Aquificales OPB13	Aquificales	17	2	—	1	—
99	1469	AF445735	Unidentified Green Non-sulfur OPB65	Green Non-Sulfur Bacteria	2	1	—	—	—
97	533	AF446260	*Dictyologlomas thermophilum*	Firmicutes (Low G + C)	1	—	—	—	—
97	662	AF446242	Cyanobacterium sp. OS type B	Cyanobacteria	1	—	—	—	—
87	700	AF446244	*Flectobacillus major*	BCF	1	—	—	—	—
98	1500	AF445689	Unidentified bacterium OPB30	β-Proteobacteria	1	3	45	51	7
				Total no. of clones in facies	68	8	62	86	8

Note: Table includes the percent similarity to previously sequenced organisms (ID%), the number of base pairs sequenced (Bp), the sequence accession number (Access.), and the best match organism in Genbank and its division. The number of 16S rRNA genes detected in each facies is indicated (V, vent facies; AC, apron and channel facies; P, pond facies; PS, proximal-slope facies; DS, distal-slope facies).

were selected for sequence analysis in an effort to capture different sequences with similar RFLP patterns. Clones selected for sequence analysis were patched onto Luria broth agar petri dishes supplemented with 200 μg/mL ampicillin (Roche Molecular Biochemicals, Indianapolis, Ind.) and incubated overnight at 37 °C.

Inoculation, cell culturing, template preparation, and sequencing were performed in the High Throughput Laboratory of the University of Illinois Urbana-Champaign W. M. Keck Center for Comparative and Functional Genomics. The petri dish cultures were used to inoculate 2 mL 96-well culture blocks containing Circle Grow media (Bio100) supplemented with ampicillin (100 μm/mL). Plasmid template DNA was purified from the cultures using an automated system and the QIAwell 96 Turbo prep BioRobot Kit (Qiagen, Valencia, Calif.). Sequencing was completed using the T7(-26) primer synthesized in-house **(**Studier and Dunn 1983**)**. Sequence reactions were performed on the plasmid templates using a Qiagen Bio Robot 9600 and Big Dye Terminator chemistry (v.2.0) from ABI. Sequencing was performed on an ABI 3700 capillary sequencer, then processed in the Bioinformatics Unit of the W. M. Keck Center.

To generate nearly complete sequences, unique clones were selected based on the sequences generated from the T7(-26) primer (Studier and Dunn 1983), and the remainder of the 16S sequence was determined using either the M13(-24) or M13(-48) primer (Viera and Messing 1982). Two other primer pairs located within the 16S rRNA gene sequence were also used. The first pair consisted of Bact343Fwd. 5′-TACGGR AGGCAGCAG and Bact 1115Rev. 5′-AGGGTTGCGCTC GTTRC (Wilmotte et al. 1993) and the second pair consisted of 805aF 5′-ATTAGATACCCYGGTAGTC and 926/20 5′-CCG TCAATTYYTTTRAGTTT (Wilmotte et al. 1993; Hugenholtz et al. 1998). Contiguous sequences were assembled manually with the DNA analysis software Sequencher 4.1 (Gene Codes Corp., Ann Arbor, Mich.).

Sequence analyses

The 16S rRNA gene sequences, determined with a 3% similarity cut-off (Martin 2002), were first compared with the GenBank database using the basic local alignment search tool (BLAST) network service (Altschul et al. 1990). From the alignments created by this search, the orientation of each cloned 16S rRNA gene could be determined and an approximate division-level association established. Each sequence was analyzed using the CHIMERA_CHECK version 2.7 program available at the Ribosomal Database Project web site (Maidik et al. 1997). Those sequences deemed to be chimeric were culled from the data set. A 97% to 100% match of the unknown clone with the GenBank data set was considered an approximate identification to the species level, 93% to 96% similarity was accepted as a genus-level identification, and an 86% to 92% match was considered a more distant yet related organism (Goebel and Stackebrandt 1994).

Nucleotide sequence accession numbers

The GenBank accession numbers for each 16S rRNA gene sequence generated in this study are listed in Tables 1 through 5.

Results

Bacterial clone 16S rRNA gene sequence libraries were constructed for each of the five travertine depositional facies at Spring AT-1. The following is a summary of the distribution of these sequences and their species-level and division-level affiliations. The number of base pairs of each 16S rRNA gene sequence, the species-level and division-level percent match with affiliated microoganisms in GenBank, and the occurrence or absence of each sequnce in each travertine depositional facies is presented in Tables 1 through 5.

16S rRNA gene sequence clone libraries

More than 14 000 clones were generated in 65 clone libraries (one per PCR reaction) from the vent, apron and channel, pond, proximal-slope, and distal-slope travertine depositional facies (Fig. 3; Tables 1–5). From this large pool, 1050 clones were selected based on their RFLP patterns and submitted to be sequenced. Ultimately, 657 clones were successfully sequenced, yielding 221 unique gene sequence types (16S rRNA gene species-level affiliations). The remaining 436 sequences were duplications of the 221 unique 16S rRNA gene sequence types. Only 6% of the bacterial gene sequences detected in the Spring AT-1 drainage system could not be assigned to a particular division (i.e., these particular 16S rRNA gene sequences differ significantly in their gene sequence from genes previously detected and recorded in the GenBank database; Tables 1–5). This similarity has permitted inferrence of bacterial affiliation and associated ecology from the Spring AT-1 sequences.

The molecular identification technique applied in this study

Table 2. 16S rRNA gene sequencing results for bacteria inhabiting the Spring AT-1 apron and channel facies.

ID%	Bp	Access.	Best match organism	Division facies	V	AC	P	PS	DS
98	1446	AF445697	Uncultured eubacterium env.OPS 1	Aquificales	—	3	4	—	—
94	424	AF446247	*Planctomyces* sp. (strain 599)	Planctomycetales	—	2	—	—	—
87	654	AF446248	Uncultured bacterium mle 1-41	Planctomycetales	—	1	—	—	—
87–88	1439	AF445645	Uncultured bacterium #0319-7F4	Planctomycetales	—	1	—	1	—
90–94	559	AF446256	Candidate division OP11 clone OPB92	OP11	—	1	14	1	—
91	610	AF446272	Uncultured bacterium, clone GR-WP33-58	Chloroplasts	—	1	—	—	—
92–94	619	AF446276	*Chlorobium ferroxidans*	Green Sulfur Bacteria	—	1	1	1	1
94	606	AF446280	*Cytophaga* sp. KT02ds22	BCF	—	1	—	—	—
89	1453	AF445737	Sphingobacterium-like sp., strain PC1.9	BCF	—	1	—	—	—
94	640	AF446285	Uncultured celluphaga SIC.B8113	BCF	—	1	—	—	—
91	593	AF446287	Unidentified cytophagales clone LD2	BCF	—	1	—	—	—
90	634	AF446291	Ultramicrobacterium str. VeSm13	Verrucomicrobium Group	—	1	—	—	—
97	600	AF446303	*Erythromonas ursinicola*	α-Proteobacteria	—	1	—	—	—
90	598	AF446311	a-Proteobacteria A0904	α-Proteobacteria	—	1	—	—	—
92	581	AF446328	Unidentified bacterium strain BD7-11	Unknown division	—	1	—	—	—
98	550	AF446331	Uncultured bacterium BHA9	Unknown division	—	1	—	—	—
94	622	AF446345	Unidentified bacterium clone 49524	Unknown division	—	1	—	—	—
				Total no. clones in facies	0	20	19	3	1

Note: See Table 1 for abbreviations.

has several potential biases (Sambrook et al. 1989; Hurst et al. 2002). These vary from the possibility of generating multiple clones of a 16S rRNA gene from any one bacterial cell in the environmental sample to failing to detect 16S rRNA gene sequences from bacteria whose cell walls are difficult to lyse for DNA extraction. In addition to this, the number of samples analyzed and PCR analyses completed in this study have been concentrated on the pond facies (Fig. 5) to eventually determine the bacterial communities associated with formation of the pond lip, which is the hallmark structural component of hot spring travertine terracette morphology. Furthermore, environmental 16S rRNA gene surveying on the scale at which it was applied in this study is time consuming and expensive. As a result of these multiple interrelated factors, the five travertine facies have not been fully molecularly *saturated* (i.e., the "true" total bacterial phylogenetic diversity has not been analytically determined), as can be shown by standard statistical analyses (data not shown; Hughes et al. 2001; Martin 2002). However, this is a problem that faces all molecular studies of bacterial diversity in the environment, and no study proposes to have determined the entire spectrum of bacterial diversity in any given natural environmental sample (Hurst et al. 2002). Therefore, the approach adopted in the present study, as in many previous studies of hot spring microbiology (e.g., Hugenholtz et al. 1996; Blank et al. 2002), has been to conduct a minimum number of PCRs to establish a reliable first-order baseline estimate of the bacterial communities inhabiting the Spring AT-1 drainage system. However, the present study has the important advantage that the analyses were conducted within the environmental framework of an independently established travertine facies model. Therefore, the resulting information on bacterial community composition has a direct physical and chemical environmental context that has not previously been known for hot spring microbial communities.

A pie chart graphical format has been chosen to depict the sequencing data in this study because phylogenetic trees are not effective in illustrating the environmental context provided by the travertine facies model (Hillis et al. 1996). Therefore, the division-level phylogenetic diversity of bacteria affiliated with the 16S rRNA gene sequences in each facies is presented in two types of pie diagrams (Fig. 4). The first type divides the number of 16S rRNA genes cloned from each bacterial division by the total number of sequences in each facies clone library (Figs. 4A, 4C, 4E, 4G, 4I). The second type divides the total number of division-level affiliations observed in the clone library by the total number of affiliated species identified in each facies (Figs. 4B, 4D, 4F, 4H, 4J). Use of these graphs permits a comparative evaluation of bacterial community composition from the total proportion of 16S rRNA gene sequences (the raw data) and the proportions of division-level identifications (the interpreted data). Both approaches are useful because neither the proportions of 16S rRNA gene sequence or species-level sequence affiliations are necessarily accurate estimates of bacterial community structure due to potential biases during PCR amplification and other laboratory manipulations (Hurst et al. 2002). Determination of the bacterial community structure and functional metabolic diversity in each facies will be completed in future studies by applying optical and molecular techniques that build directly upon the 16S rRNA gene sequence clone libraries constructed in this study (Tables 1–5).

Microbial communities inhabiting the vent facies

The vent facies clone libraries were dominated by bacterial sequences affiliated with *Aquificales* (91% sequences, 29% 16S rRNA gene types; Table 1; Figs. 6A, 6B). The observed discrepancy between total number of gene sequences and the total number of unique affiliated 16S rRNA gene types (Figs. 6A, 6B) presumably represents the preferential amplification of *Aquificales* 16S rRNA gene sequences during PCR. More than 40% of the total 16S rRNA gene types detected

Table 3. 16S rRNA gene sequencing results for bacteria inhabiting the Spring AT-1 pond facies.

ID%	Bp	Access.	Best Match Organism	Division facies	V	AC	P	PS	DS
92	607	AF446246	Candidate division OP8 clone OPB23	OP 8	—	—	1	—	—
89–93	1479	AF445727	*Pirellula staleyi* (strain DSM 6068T)	Planctomycetales	—	—	7	—	—
92	267	AF446249	*Chloroflexus* sp., HS-7	Green Non-Sulfur Bacteria	—	—	1	—	—
93	564	AF446250	*Chloroflexus aurantiacus*	Green Non-Sulfur Bacteria	—	—	1	—	—
94	1484	AF445701	Uncultured bacterium sp. oral clone BE109	Candidate division TM7	—	—	1	—	—
84	263	AF446253	Candidate division OP11 clone OPd29	OP11	—	—	1	—	—
98	1474	AF445690	Candidate division OP11 clone NTd42	OP11	—	—	1	1	—
94–95	527	AF446254	Candidate division OP11 clone OPd47	OP11	—	—	2	—	—
95–98	1476	AF445687	Candidate division OP11 Clone OPB92	OP11	—	—	9	—	—
93–97	606	AF446257	Candidate division OP11 clone OPB92	OP11	—	—	8	—	1
98–99	1473	AF445644	Thermus YSPID A.1	Thermus-Deinococcus Group	—	—	4	1	—
94	1500	AF445685	*Paenibacillus larvae* subsp. pulvifaciens	Firmicutes (Low G + C)	—	—	1	—	—
99	632	AF446261	*Paenibacillus* sp. Isolate TOD45	Firmicutes (Low G + C)	—	—	1	—	—
93	612	AF446262	Uncultured eubacterium OPI-6	Firmicutes (Low G + C)	—	—	1	—	—
96–99	1484	AF445745	Eubacterium sp. (OS type L)	Firmicutes (Low G + C)	—	—	4	—	—
97	1486	AF445720	Eubacterium strain OS type L	Firmicutes	—	—	1	—	—
97	592	AF446263	*Oscillatoria neglecta*	Cyanobacteria	—	—	1	—	—
98–99	545	AF446264	*Planktothrix* sp. FP1	Cyanobacteria	—	—	3	—	—
95	480	AF446265	*Planktothrix* sp. FP1	Cyanobacteria	—	—	2	—	—
97–99	1448	AF445707	*Spiruilina* sp., strain CCC Snake P. Y-85	Cyanobacteria	—	—	1	7	2
99	1432	AF445722	Synechococcus sp. ATCC 700246	Cyanobacteria	—	—	16	12	3
89	1446	AF445691	*Synechococcus* sp. PCC 7902	Cyanobacteria	—	—	1	7	—
97	600	AF446243	Cyanobacterium sp. OS type B	Cyanobacteria	—	—	1	—	—
92–93	379	AF487343	*Mesostigma viride* chloroplast	Chloroplasts	—	—	1	—	—
87–91	600	AF446269	*Cyanophora paradoxa* cyanelle	Chloroplasts	—	—	7	—	—
87–90	216	AF446270	*Nephroselmis olivacea* chloroplast	Chloroplasts	—	—	3	—	—
92	486	AF446271	Unidentified eukaryote OM81	Chloroplasts	—	—	1	—	—
88	1436	AF445704	*Prosthecochloris aestuarii*	Green Sulfur Bacteria	—	—	1	—	—
99	1507	AF445702	Unidentified green sulfur bacterium OPS77	Green Sulfur Bacteria	—	—	1	—	—
91–92	620	AF446290	*Dyadobacter fermentens*	BCF	—	—	2	—	—
84	659	AF446282	*Flectobacillus* sp., strain MWH38	BCF	—	—	2	—	—
90	1483	AF445721	*Haliscomenobacter hydrossis* ATCC27775	BCF	—	—	1	—	—
95	424	AF446283	*Lewinella nigricans*	BCF	—	—	1	—	—
93	1468	AF445698	Spirosoma-like sp. (strain PC5.1A)	BCF	—	—	1	—	—
94	1483	AF445684	Uncultured Cytophagales bacterium clone 13	BCF	—	—	3	1	—
84	266	AF446286	uncultured cytophaga 67C12	BCF	—	—	1	—	—
99	637	AF446288	Unidentified Cytophagales OPB73	BCF	—	—	1	—	—
95–97	687	AF446289	Uncultured bacterium CLEAR-1	BCF	—	—	3	—	—
90	1482	AF445681	Uncultured bacterium EKHO-12	BCF	—	—	2	—	—
92–93	563	AF446290	Uncultured bacterium GKS2–164	BCF	—	—	3	—	—
90	1422	AF445718	Uncultured Verrucomicrobium DEV008	Verrucomicrobium Group	—	—	1	—	—
86	424	AF446292	*Bdellovibrio bacteriovorus* (Strain SRA9)	δ-Proteobacteria	—	—	1	—	—
90	1471	AF445705	*Bdellovibrio bacteriovorus* strain BRP4	δ-Proteobacteria	—	—	1	1	—
91	1460	AF445695	*Bdellovibrio bacteriovorus* strain BRP4	δ-Proteobacteria	—	—	1	—	—
92	415	AF446294	*Polyangium vitellinum*	δ-Proteobacteria	—	—	1	—	—
99	1447	AF445742	*Blastobacter denitrificans*	α-Proteobacteria	—	—	1	—	—
99	596	AF446296	*Brevundimonas* sp., strain FWC04	α-Proteobacteria	—	—	1	—	—
98	600	AF446297	*Brevundimonas* sp., strain FWC43	α-Proteobacteria	—	—	2	—	—
98	516	AF446299	*Brevundimonas alba*, strain CB88	α-Proteobacteria	—	—	1	—	—
99–100	409	AF446300	*Brevundimonas bacteroides*, strain CB7	α-Proteobacteria	—	—	1	2	—
99	611	AF487342	*Brevundimonas variablis*	α-Proteobacteria	—	—	11	—	—
97	1430	AF445680	*Devosia riboflavina* (strain:IFO 13584)	α-Proteobacteria	—	—	1	—	—
95	1414	AF445717	*Hyphomonas jannaschiana*, strain ATCC 33883 (T)	α-Proteobacteria	—	—	1	—	—
99	566	AF446304	*Hyphomonas rosenbergii*	α-Proteobacteria	—	—	1	—	—
95	610	AF446305	*Mesorhizobium* sp. USDA 3466	α-Proteobacteria	—	—	1	—	—
99	654	AF446307	*Porphyrobacter* sp. KK351	α-Proteobacteria	—	—	1	—	—
96	565	AF446309	*Rhodobacter sphaeroides*	α-Proteobacteria	—	—	1	—	—
95	1412	AF445668	*Rubrimonas cliftonensis* (strain: OCh317)	α-Proteobacteria	—	—	4	2	—
96	558	AF446313	Alpha-proteobacterium TV6–2b	α-Proteobacteria	—	—	1	—	—
94	1498	AF445686	*Lysobacter antibioticus* DSM 2044	γ-Proteobacteria	—	—	1	—	—
95–96	537	AF446314	Gamma-proteobacteria MBIC 3957	γ-Proteobacteria	—	—	2	—	—
95	1504	AF445683	Uncultured bacterium, clone BIsiii14	γ-Proteobacteria	—	—	6	—	—
94	1505	AF445723	unidentified bacterium (strain: rJ15)	γ-Proteobacteria	—	—	3	—	—

Table 3 (*concluded*).

ID%	Bp	Access.	Best Match Organism	Division facies	V	AC	P	PS	DS
99	1488	AF445688	*Hydrogenophaga palleronii*	β-Proteobacteria	—	—	3	—	—
0.995	1483	AF445700	*Pseudomonas saccharophila* DSM 654T	β-Proteobacteria	—	—	1	—	—
98	504	AF446315	*Rubrivivax gelatinosus* (strain IL144)	β-Proteobacteria	—	—	1	—	—
99	407	AF446316	*Tepidimonas ignava*	β-Proteobacteria	—	—	1	—	—
98–99	506	AF446317	beta-proteobacterium OS-ac-15	β-Proteobacteria	—	—	4	—	—
97	1482	AF445694	Unidentified Bacteria (strain:HW1)	β-Proteobacteria	—	—	1	—	—
96	1499	AF445699	Acid-degrading bacterium DhA-73	β-Proteobacteria	—	—	4	—	1
97–98	467	AF446318	Unidentified b-proteobacterium OPS63	β-Proteobacteria	—	—	2	1	—
95	447	AF446319	Grassland soil clone saf1_110	Unknown division	—	—	1	—	—
93–94	564	AF446320	rhizospere soil bacterium RSC-II-42	Unknown division	—	—	5	—	—
89	624	AF446321	Uncultured soil bacterium C011	Unknown division	—	—	4	—	—
89	412	AF446322	Uncultured soil bacterium S0212	Unknown division	—	—	1	—	—
88	601	AF446324	potato plant root bacterium RC-III-43	Unknown division	—	—	2	—	—
94	295	AF446325	potato plant root bacterium RC-III-57	Unknown division	—	—	1	—	—
96	338	AF446326	maize root bacterium ZmrIs6	Unknown division	—	—	1	—	—
90	1437	AF445724	alpha proteobacterium 34614	Unknown division	—	—	1	—	—
94	1476	AF445725	*Lysobacter antibioticus* DSM 2044	Unknown division	—	—	1	—	—
91	432	AF446329	Unidentified bacterium BD5–13	Unknown division	—	—	1	—	—
84	596	AF446330	Unidentified bacterium BD5–13	Unknown division	—	—	2	—	—
96	601	AF446333	Uncultured hot spring bacterium GFP1	Unknown division	—	—	1	—	—
98	522	AF446334	Unidentified eubacterium clone GKS16	Unknown division	—	—	1	—	—
91–92	418	AF446335	Unidentified bacterium ID SBR 1034	Unknown division	—	—	1	1	—
90–91	563	AF446339	OPB56	Unknown division	—	—	2	—	—
99	624	AF446340	OPB56	Unknown division	—	—	1	—	—
86	1477	AF445703	Uncultured bacterium PHOS-HD29	Unknown division	—	—	1	—	—
93–95	627	AF446341	Unidentified bacterium strain rJ15	Unknown division	—	—	5	—	—
91	1441	AF445692	Uncultured Bacterium SJA-35	Unknown division	—	—	5	5	—
95	598	AF446343	Unknown bacterium TBJ001345	Unknown division	—	—	5	—	—
95	1482	AF445700	Bacterial clone 11–25 (new phylum?)	Unknown division	—	—	1	—	—
				Total no. clones in facies	0	0	208	41	7

Note: See Table 1 for abbreviations.

in the vent facies also occurred in the other four downstream depositional facies, with large numbers of sequences affiliated with uncultured *Aquificales* pBB detected in the pond and proximal-slope facies (Table 1). Vent facies bacterial sequences representing β-proteobacteria were detected in all four downstream facies, with the largest number in the proximal-slope facies (Table 1). The vent facies clone library contained no sequences or 16S rRNA gene types with unknown affinity (Figs. 6A, 6B).

Microbial communities inhabiting the apron and channel facies

Clone libraries from the apron and channel facies were affiliated with a higher diversity bacterial assemblage (10 divisions, 21 16S rRNA gene types) than the vent facies (6 divisions, 7 16S rRNA gene types; Figs. 6C, 6D; Table 2). An equal number of PCR reactions were run for the vent and apron channel facies, respectively, (Fig. 5). Libraries from the apron and channel facies were dominated by sequences affiliated with *Aquificales* (Figs. 6C, 6D), which were lower in abundance than those detected in the vent facies (Figs. 6A, 6B). Approximately 33% of the 16S rRNA gene types occurring in the apron and channel facies were identified in the other three downstream facies, while nearly 20% of the apron and channel 16S rRNA gene types were observed in the upstream vent facies (Table 2). The apron and channel facies clone library contained 11% sequences and 14% 16S rRNA gene types with unknown affinity (Figs. 6C, 6D).

Microbial communities inhabiting the pond facies

The pond facies contained bacterial clone library sequences that were affiliated with 17 bacterial divisions (Table 3). This is the highest bacterial diversity recorded for any of the five Spring AT-1 travertine depositional facies (Figs. 5, 6). Nearly five times more PCRs were conducted on the pond facies than either the vent or apron channel facies (Fig. 5). While this increase in PCRs is expected to increase the number of sequences that are detected, it is unlikely that this effect accounts for all of the dramatic increase observed in pond facies division-level sequence diversity. Supporting evidence for this assertion is that the RFLP patterns used to discriminate clones exhibited little variation in the vent and apron and channel facies but significantly higher variability in the pond and proximal-slope facies. The pond facies clone library was dominated by sequences affiliated with β-*Proteobacteria*, while the 16S rRNA gene types predominantly represented α-*Proteobacteria* (Figs. 6E, 6F). Other abundant clones in the pond facies library were affiliated with divisions OP 11 and BCF (*Bacteroides, Cytophagales, and Flexibacter*; Figs. 6E, 6F). The pond facies clone library contained the largest proportion of 16S rRNA gene types with unknown affinity in the Spring AT-1 drainage system (Figs. 6E, 6F).

Microbial communities inhabiting the proximal-slope facies

Clone libraries from the proximal-slope facies also exhibited extremely high diversity, containing sequences representing 16 bacterial divisions (Table 4). The number of PCRs con-

Table 4. 16S rRNA gene sequencing results for bacteria inhabiting the Spring AT-1 proximal-slope facies.

ID%	Bp	Access.	Best match organism	Division facies	V	AC	P	PS	DS
97	1441	AF445672	*Heliothrix oregonensis* (strain F1)	Green Non-Sulfur Bacteria	—	—	—	1	—
95	1437	AF445666	*Roseiflexus castenholzii* (strain: HLO8)	Green Non-Sulfur Bacteria	—	—	—	1	—
91	401	AF446251	Uncultured eubacterium WCHB1–50	Green Non-Sulfur Bacteria	—	—	—	2	—
83	506	AF446252	Uncultured bacterium ACE-27	OP11	—	—	—	1	—
86-88	285	AF446255	Candidate division OP11 clone OPB92	OP11	—	—	—	2	—
90	401	AF446258	*Thermus brockianus*, strain 15038T	Thermus-Deinococcus Group	—	—	—	1	—
91	468	AF446259	Uncultured actinobacterium 420ev	Actinomycetes	—	—	—	1	—
92	580	AF446266	*Pseudoanabaena* PCC6903	Cyanobacteria	—	—	—	1	—
98	1447	AF445678	Spirulina sp. strain CCC Snake P. Y-85	Cyanobacteria	—	—	—	1	—
83	267	AF446267	*Synechococcus* sp., strain PCC7003	Cyanobacteria	—	—	—	1	—
99.6	1445	AF445654	Synechococcus ATCC700244	Cyanobacteria	—	—	—	1	—
99	256	AF446268	*Synechococcus* ATCC 700245	Cyanobacteria	—	—	—	6	—
86	1445	AF445677	*Synechococcus* PCC9005	Cyanobacteria	—	—	—	1	—
99	1475	AF445656	*Juniperus virginiana* chloroplast	Chloroplasts	—	—	—	1	—
88	1454	AF445662	*Chlorobium limicola* (Y10113)	Green Sulfur Bacteria	—	—	—	11	—
93–94	492	AF446277	*Chlorobium tepidum*	Green Sulfur Bacteria	—	—	—	4	—
89–90	510	AF446278	*Pelodictyon luteolum*	Green Sulfur Bacteria	—	—	—	2	—
93	510	AF446279	*Pelodictyon luteolum*	Green Sulfur Bacteria	—	—	—	2	—
97	1437	AF445706	Uncultured bacterium	Green Sulfur Bacteria	—	—	—	1	—
98	1272	AF445663	Uncultured bacterium	Green Sulfur Bacteria	—	—	—	1	—
88	1469	AF445665	*Flexibacter elegans*	BCF	—	—	—	1	—
89	1479	AF445661	*Sporocytophaga myxococcoides* DSM 11118T	BCF	—	—	—	1	—
88	1453	AF445730	Sphingobacterium-like sp. (strain PC1.9)	BCF	—	—	—	2	—
88	1471	AF445648	Uncultured bacterium clone Ebpr17	BCF	—	—	—	1	—
93	1443	AF445647	Uncultured CFB group bacterium kpj59rc	BCF	—	—	—	9	—
93	1429	AF445660	Uncultured CFB group bacterium kpj59rc	BCF	—	—	—	2	—
89	895	AF445708	*Leptospira fainei*, SSI 5402–98	Spirochetes	—	—	—	1	—
93	544	AF446293	*Desulfovibrio* sp. (clone B4)	δ-Proteobacteria	—	—	—	1	—
91	457	AF446295	Delta proteobacterium S2551	δ-Proteobacteria	—	—	—	1	—
91	1429	AF445733	Uncultured bacterium, clone P2E10	δ-Proteobacteria (?)	—	—	—	3	—
91	1435	AF445743	Unidentified bacterium, strain BD1–5	ϵ-Proteobacteria	—	—	—	1	—
96	351	AF446301	*Caulobacter crescentus*	α-Proteobacteria	—	—	—	1	—
90	390	AF446302	*Caulobacter* sp., strain FWC21	α-Proteobacteria	—	—	—	1	—
99	1336	AF445710	*Porphyrobacter* sp. KK348	α-Proteobacteria	—	—	—	7	—
99	1444	AF445711	*Porphyrobacter* sp. KK348	α-Proteobacteria	—	—	—	1	—
98	379	AF446308	*Porphyrobacter* sp. MBIC3897	α-Proteobacteria	—	—	—	1	—
91	1419	AF445674	*Rhizobium yanglingense* CCBAU71462	α-Proteobacteria	—	—	—	1	—
88	1459	AF445655	*Rickettsia montanensis*	α-Proteobacteria	—	—	—	1	—
96	1446	AF445713	*Caulobacter* sp. type V, strain CB28	α-Proteobacteria	—	—	—	1	—
97	1420	AF445712	*Spingomonas asaccharolytica*	α-Proteobacteria	—	—	—	2	—
90	1442	AF445675	Alpha proteobacterium MBIC3401	α-Proteobacteria	—	—	—	1	—
87	1456	AF445649	Uncultured marine eubacterium HstpL69	α-Proteobacteria	—	—	—	1	—
91	1437	AF445669	Uncultured bacterium clone 4-Org2-22	α-Proteobacteria	—	—	—	3	—
88	1489	AF445671	*Stenotrophomonas maltophilia* LMG 10877	γ-Proteobacteria	—	—	—	2	—
98	332	AF446323	Unidentified soil bacterium	Unknown division	—	—	—	1	—
90	1465	AF445646	Unidentified bacterium OPB56	Unknown division	—	—	—	1	—
88	1447	AF445744	*Lactobacillus sanfranciscensis*ATCC 27651 T	Unknown division	—	—	—	2	—
95	1437	AF445666	*Roseiflexus castenholzii* (strain: HLO8)	Unknown division	—	—	—	1	—
93	1438	AF445709	Uncultured bacterium, clone BIfdi48	Unknown division	—	—	—	1	—
96	248	AF446332	Uncultured eubacterium CR-PA13	Unknown division	—	—	—	1	—
88	1448	AF446738	Uncultured Antarctic bacterium LB3–100	Unknown division	—	—	—	2	—
93	406	AF446337	Unidentified bacterium, (OS) type E	Unknown division	—	—	—	1	—
98	407	AF446338	Unidentified bacterium, (OS) type E	Unknown division	—	—	—	1	—
89	1481	AF445650	Uncultured bacterium PHOS-HD29	Unknown division	—	—	—	1	—
90	1454	AF445676	Uncultured sludge bacterium S14	Unknown division	—	—	—	1	—
91	433	AF446342	Uncultured bacterium SY1–54	Unknown division	—	—	—	1	—
90	1460	AF445657	Unidentified bacterium clone 4955	Unknown division	—	—	—	1	—
				Total no. clones in facies	0	0	0	103	0

Note: See Table 1 for abbreviations.

Table 5. 16S rRNA gene sequencing results for bacteria inhabiting the Spring AT-1 distal-slope facies.

ID%	Bp	Access.	Best match organism	Division facies	V	AC	P	PS	DS
96	560	AF446241	Uncultured eubacterium env. OPS 7	Aquificales	—	—	—	—	1
95	1467	AF445715	Uncultured bacterium clone SL35	Planctomycetales	—	—	—	—	1
90	1442	AF445719	*Synechococcus elongatus*	Cyanobacteria	—	—	—	—	2
94	1427	AF445714	Unidentified rhodophyte PRD01a010B	Chloroplasts	—	—	—	—	2
84	405	AF446273	*Chrysodidymus synuroideus* mitochondria	Eukaryota, Mitochondria	—	—	—	—	1
88–90	409	AF446274	*Chrysodidymus synuroideus* mitochondria	Eukaryota, Mitochondria	—	—	—	—	2
92	311	AF446275	*Chrysodidymus synuroideus* mitochondria	Eukaryota, Mitochondria	—	—	—	—	1
95	221	AF446284	*Runella slithyformis*	BCF	—	—	—	—	1
90	1461	AF445716	*Acidomonas methanolica* IMET10945	α-Proteobacteria	—	—	—	—	2
98	405	AF446298	*Brevundimonas alba*, strain CB88	α-Proteobacteria	—	—	—	—	1
93	405	AF446306	*Paracoccus*, isolate B8B1	α-Proteobacteria	—	—	—	—	1
95	570	AF446245	*Rhodobacter sp*. (strain TCRI 3)	α-Proteobacteria	—	—	—	—	1
88	611	AF446310	*Rickettsia massiliae*	α-Proteobacteria	—	—	—	—	1
95	338	AF446312	Alpha-proteobacterium A0904	α-Proteobacteria	—	—	—	—	1
95	539	AF446346	Grassland soil clone saf2_421	Unknown division	—	—	—	—	1
92	339	AF446327	Uncultured maize root bacterium Zmrc235	Unknown division	—	—	—	—	1
93	1479	AF445728	Uncultured bacterium, clone BIfdi48	Unknown division (GS, BCF)	—	—	—	—	1
95	453	AF446344	Uncultured bacterium TRA1–20	Unknown division	—	—	—	—	1
				Total no. clones in facies	0	0	0	0	22

Note: See Table 1 for abbreviations.

ducted on the proximal-slope facies is comparable to the number of reactions run on the pond facies (Fig. 5). Therefore, the affiliated bacterial diversity in the proximal-slope facies can be directly compared with the pond facies. As was the case in the pond facies, the proximal-slope facies clone library was dominated by sequences affiliated with β-*Proteobacteria*, while the 16S rRNA gene types predominantly represented α-*Proteobacteria* (Figs. 6G, 6H). Other important clones in the proximal-slope facies library were affiliated with *Cyanobacteria*, *Aquificales*, and BCF (Figs. 6G, 6H). The proximal-slope facies clone library contained the largest proportion of sequences with unknown affinity (Figs. 6G, 6H).

Microbial communities inhabiting the distal-slope facies

Only three PCRs were run on samples collected from the distal-slope facies (Fig. 5). Therefore, although it is known that the bacterial diversity in the distal-slope facies has been significantly underestimated due to the small number of PCRs, this initial molecular survey has provided a useful evaluation of the extent of bacterial community partitioning and a preliminary estimate of the phylogentic diversity in the facies. Fewer analyses were performed in the distal-slope facies because it was assumed that (1) the bacterial phylogenetic diversity would be significantly greater at lower water temperatures; and (2) "wash through" of bacteria from the higher temperature facies would be significant and therefore complicate interpretations of the bacterial communities. Results suggest that neither assumption was accurate for the Spring AT-1 drainage system. The distal-slope facies clone library contained 11% sequences and 18% 16S rRNA gene types with unknown affinity (Table 3; Figs. 5, 6I, 6J). While dominated by sequences affiliated with α-*Proteobacteria*, the libraries also contained clones affiliated with 8 bacterial divisions including β-*Proteobacteria* and *Cyanobacteria* (Figs. 6I, 6J).

Discussion

The distribution of 16S rRNA gene sequences detected in this study indicate that bacteria are distinctly partitioned among the five travertine depositional facies composing the Spring AT-1 drainage system (Fig. 2). The percentage of 16S rRNA gene types found exclusively within each facies are vent facies 43%, apron and channel facies 64%, pond facies 80%, proximal-slope facies 79%, and distal-slope facies 79% (Tables 1–5). For the Spring AT-1 drainage system as a whole, 88% of the 657 gene sequences and 77% of the 221 16S rRNA gene types were found in only one of the five facies (Tables 1–5). The following discussion evaluates the implications of this bacterial partitioning with respect to downstream transport, microbial ecology, and travertine precipitation.

Downstream transport

The strong facies-specific partitioning of bacterial gene sequences implies that relatively little (≤~25%) downstream transport of bacterial cells occurs despite the constant flow of water across the Spring AT-1 drainage system (Fouke et al. 2000). The high level of partitioning also argues against the uncertainties created by not knowing (1) the complete bacterial phylogenetic diversity of each facies; (2) whether the bacteria affiliated with the 16S rRNA sequences detected in this study were alive or dead at the moment they were collected; and (3) exactly what proportion of the bacterial cells may have been washed downstream from upstream facies (Fig. 2). Therefore, the bacteria affiliated with gene sequences detected in this study are interpreted to have been normal in situ inhabitants of each facies. Downstream cell transport may take place via cell movement and gliding within substrate biofilms and microbial mats, cell suspension in the water column, and cell attachment to H_2O molecules that rise as steam from the water–air interface (aerosolization; Bonheyo et al. 2000). It is possible that higher proportions of down-

Fig. 5. Histogram summary of the molecular microbiology analyses completed in the Spring AT-1 travertine depositional facies, including number of gene sequences, inferred 16S rRNA gene types, polymerase chain reactions (PCRs), and affiliated divisions. The total number of physical samples and PCRs leading to clone libraries is indicated for each facies. Each physical sample from the spring was treated using multiple DNA extraction methods and multiple PCRs (described in the Methods section).

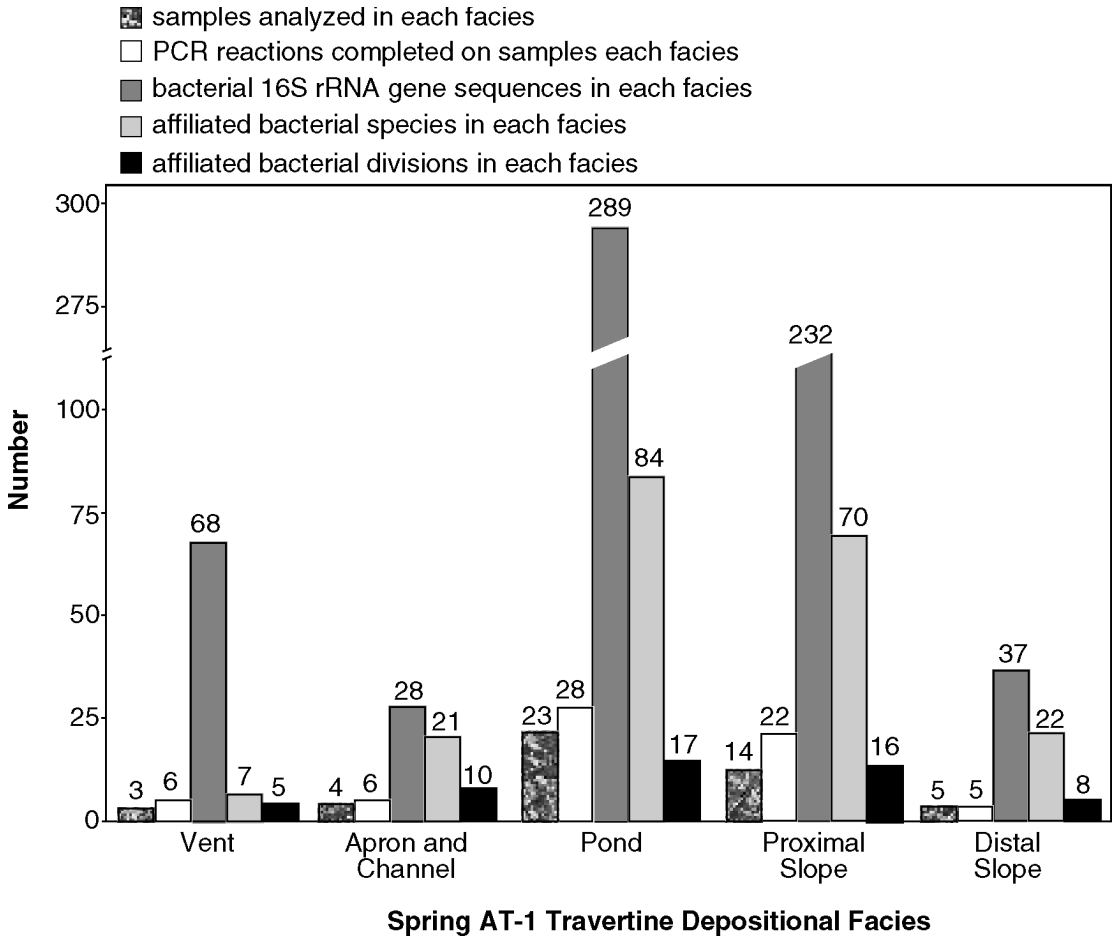

stream bacterial transport are occurring, but at levels below detection.

Seasonal monitoring of the Spring AT-1 drainage system indicates that the travertine depositional facies and their associated bacterial communities are systematically reestablished in days or weeks over lateral distances of up to a few metres (Fouke et al. 2000). This occurs in response to shifts in vent position, fluctuations in water discharge and flow rate, and (or) the emergence of new spring vents. The successful colonization of new substrate after each shift of the spring drainage system requires that the bacterial cells in the new flow paths are viable and actively multiply. An alternative to bacterial transport is the hypothesis that "everything is everywhere and the environment selects" (Brock et al. 2001). This concept was first introduced by Bass-Becking in 1935, who concluded that the energetics of phototrophy and chemolithotrophy require that the distribution of bacteria utilizing these metabolisms are controlled by the geochemical composition of the water in which they live (Brock et al. 2001). If bacterial cells are everywhere and in all environments, then the observed facies-specific partitioning of bacteria in Spring AT-1 is triggered by, and therefore even more directly reflects, the systematic changes in water physical and chemical conditions that take place along the drainage system (Fig. 2A and B; Fouke et al. 2000).

Microbial ecology

The presence or absence of bacteria is directly controlled by hot spring physical and chemical environmental conditions, which include parameters such as water temperature, flow rate, pH, light, and nutrient availability (Pace 1997; Brock et al. 2001). In turn, bacteria manipulate the surrounding physical and chemical aqueous environment, to varying degrees, via their metabolic activity and physical presence (Pace 1997; Brock et al. 2001). From a geological perspective, this feedback system ultimately controls the ability of bacteria to influence carbonate crystal precipitation. Therefore, tracking these interactions in modern hot spring travertine facies may eventually permit, in future studies, the reconstruction of the ecology and diversity of ancient bacteria from fossilized terrestrial hot spring sedimentary deposits.

The present approach of conducting molecular analyses within a travertine facies model is a first step toward a process-oriented understanding of these bacteria, water, and carbonate crystal interactions. Previous microbiological work in terrestrial and marine hot spring systems has focused on the phylogenetic

Fig. 6. Pie diagrams illustrating the division-level diversity of the partial 16S rRNA bacterial sequences composing the clone libraries derived from each facies. The clone library data is presented in two different ways for each facies. The first is a pie diagram showing the division-level proportion of the total number of gene sequences (raw data) representing each division. The second is a pie diagram showing the division-level proportion of 16S rRNA gene types (interpreted data) representing each division.

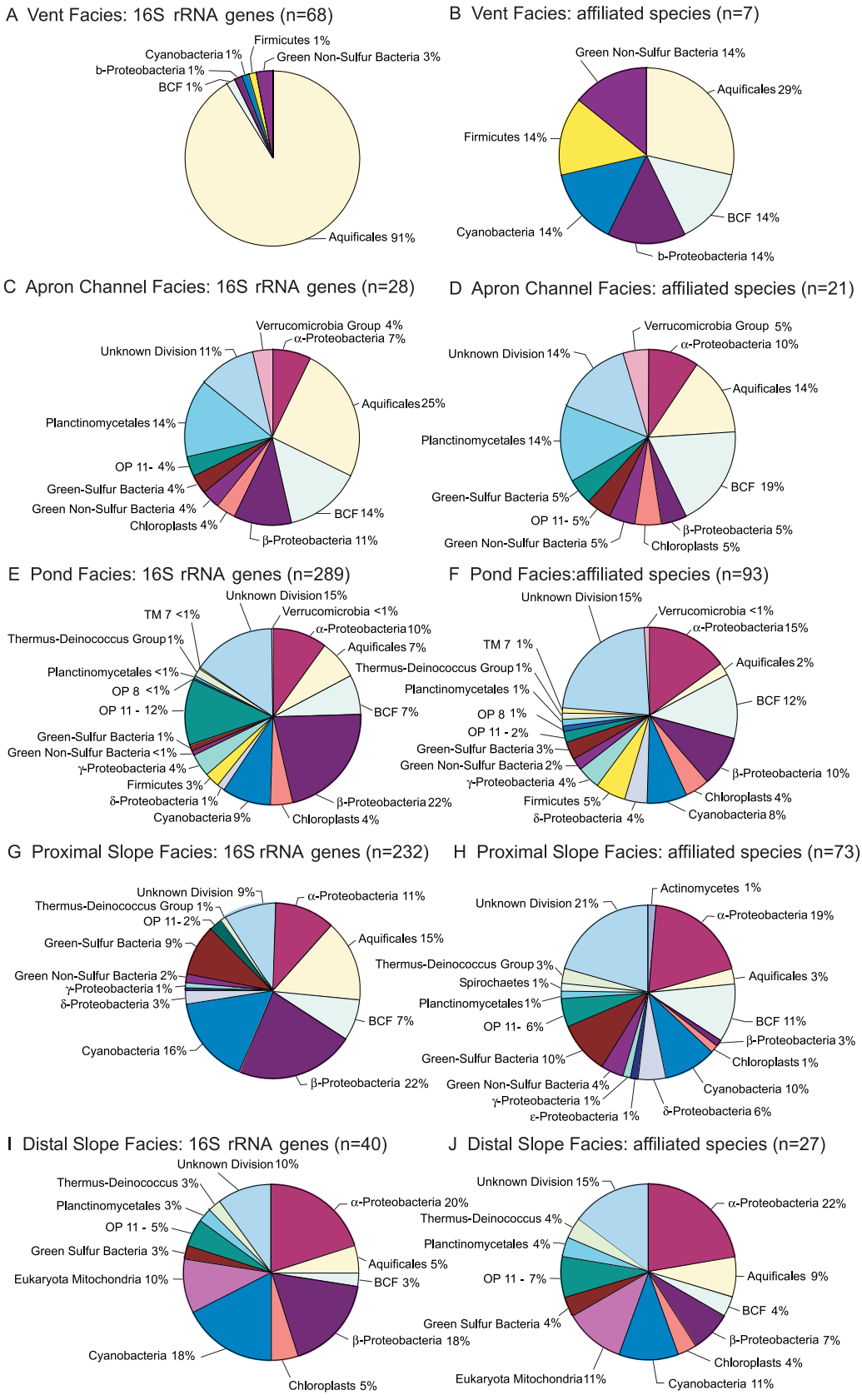

diversity of thermophilic bacteria and archea (Stahl et al. 1985; Ward et al. 1998; Hugenholtz et al. 1998; Reysenbach et al. 1999; Huber et al. 2002; Blank et al. 2002). These pioneering studies have revolutionized our knowledge of the diversity of microbial life on this planet (Woese 1987; Pace 1997; Whitman 1998). However, because much of this work has focused exclusively on demonstrating microbial diversity, the molecular analyses have generally not been linked with rigorous environmental analyses. Therefore, relatively little is known of the ecological and geological context of thermophilic and mesophilic bacterial life in hot springs (Skirnisdottir et al. 2000).

The extremely high facies-specific partitioning of bacterial 16S rRNA gene sequences observed in this study indicates that bacterial communities are themselves a sensitive biological indicator of environmental physical and chemical conditions. Specific environmental conditions, called *niches*, are required for a bacterium to grow. These include the availability of nutrients, interactions with other organisms, and the physical and chemical conditions of the water in which they live (Brock et al. 2001). While every bacterium inhabits a prime niche in which it is most successful, most bacteria can also inhabit other niches in which they are less successful (Brock et al. 2001). Sequences affiliated with *Aquificales*, β-*Proteobacteria*, and *Green Non-Sulfur* bacteria from the high-temperature vent facies were detected in downstream lower temperature facies, as well as in the vent (Table 1). This particular suite of autotrophic thermophiles may be able to tolerate extreme changes in temperature, pH, pCO_2, nutrient availability, and flow rate conditions that are outside of their prime niche. It is also possible that at least some of the detected gene sequences were washed down from upstream facies. However, the high proportion of facies-specific sequences detected in this study indicates that the majority of bacteria inhabiting the Spring AT-1 outflow have a prime niche that is equivalent to the nutrient availability and environmental conditions present in each travertine depositional facies.

An example of a bacterium with a broad niche is *Aquificales* pBB, which was the most abundant bacterial sequence in the vent facies clone library (Table 1). This unique uncultured strain occurred in all downstream depositional facies and thus may have an extremely wide range of environmental tolerance if the downstream facies contained living viable cells. It has previously been observed in deep-sea hydrothermal vents on the Mid-Atlantic Ridge (112 °C and pH 6, Reysenbach et al. 2000*a*). Closely related aquificales sequences have also been reported from Calcite Springs in Yellowstone National Park (83 °C and pH 7.6, Reysenbach et al. 2000*b*) and terrestrial siliceous hot springs in Iceland (65–70 °C and pH 8.3, Skirnisdottir et al. 2000; 79–83 °C and pH 8.8, Takacs et al. 2002). Vent facies sequences affiliated with *Aquificales* OPB13, *Green Non-Sulfur* OPB65, and β-*Proteobacterium* OPB30 (Table 1) have been reported from Obsidian Pool on the northern flank of the Yellowstone caldera (Hugenholtz et al. 1998). Obsidian Pool contains 75–95 °C siliceous waters that are rich in reduced iron, sulfide, CO_2, and hydrogen (Hugenholtz et al. 1998). These conditions are significantly different from the physical and chemical environment of Spring AT-1 (Fouke et al. 2000). The cyanobacterium OS type B was detected in Octopus Spring, which is also a 48–72 °C siliceous pool in the lower Yellowstone National Park geyser basin (Ferris et al. 1996). The BCF bacterium *Flectobacillus major* in the Spring AT-1 vent facies has been reported from siliceous hot springs in Antarctic lakes and Japan (Suzuki et al. 2001).

Travertine precipitation

The partitioning of microbes within depositional facies along the Spring AT-1 drainage system (Tables 1–5) indicates that there are systematic correlations between the composition of bacterial communities and the water chemistry, travertine chemistry, and travertine morphology described in Fouke et al. (2000). The facies-specific 16S rRNA gene libraries identified in the present study set the stage for future studies that will use integrated molecular 16S rRNA gene and optical analytical tools to correlate the presence and activity of individual bacterial species with specific travertine crystal growth forms and chemistries.

Although the potential results of these types of studies are extremely promising, specific interactions between bacteria and carbonate crystal precipitation are extremely complicated and will be challenging to identify. As an example, it is generally hypothesized that the consumption of CO_2 by photosynthetic autotrophs is capable of driving extracellular carbonate precipitation. However, recent work indicates that the PxcA protein in the plasma membrane of photosystem II cyanobacteria may significantly lower the pH of the outer cell membrane (Zak et al. 2001). The activity of this protein could, therefore, prevent extracellular carbonate mineralization even during active photosynthesis and CO_2 consumption. Therefore, a biofilm or mat of cyanobacteria could either positively, neutrally, or negatively affect travertine crystal nucleation and growth (Beveridge 1988; Vasconcelos et al. 1997; Newman et al. 1997). Furthermore, the thickest cyanbacterial mats occur in the pond and proximal-slope facies where travertine precipitation is the most rapid. This may imply that bacteria somehow attenuate or limit crystal nucleation on their outer cell walls.

A unique environmental context of the microbes inhabiting Spring AT-1 is that they must cope with extremely high rates of travertine precipitation, which reach 5 mm/day at the margin of the pond facies (Fig. 2; Fouke et al. 2000). To survive this rapid crystallization, microbes must restrict precipitation as their cells migrate to the top of the encrusting crystals or rapidly divide and laterally colonize new substrates to remain a step ahead of crystal entombment and resulting cell death. For the bacteria whose cell walls form crystallization substrates, the race to escape crystal entombment will have significant influence on the shape and perhaps chemical composition of the associated travertine deposits. This is consistent with previous observations in eutrophic lakes indicating that bacterial filament formation is a growth rate-controlled defense mechanism against grazing by eukaryotes (Hahn et al. 1999). In the case of Spring AT-1, the high rates of travertine crystallization may be an analogous environmental pressure to that of predation with respect to filamentous growth morphology. A striking example of this process is the formation of hollow aragonite "streamers" in the vent and apron and channel facies (Farmer and Des Marais 1994 Fouke et al. 2000; Farmer 2000). Aquificales cells move or divide laterally within filamentous sheaths at rates slightly higher than the

rate of crystal precipitation, forming the aragonite streamer crystalline morphology.

Conclusions

The 16S rRNA diversity of terrestrial hot spring bacteria has been mapped within travertine depositional facies comprising the Spring AT-1 drainage system at Angel Terrace, Mammoth Hot Springs, Yellowstone National Park. This has permitted direct correlation of the distribution of bacterial communities with systematic changes in spring water conditions and travertine crystal morphology and chemistry. For the Spring AT-1 drainage system as a whole, a remarkable 88% of 657 gene sequences and 77% of 221 16S rRNA gene types were found in only one of the five travertine depositional facies. Therefore, relatively little (≤~25%) downstream transport of bacterial cells occurs despite the constant flow of water across the surface of the Spring AT-1 drainage system. These results indicate that the aqueous environmental conditions defining each travertine depositional facies are also the dominant controls on microbial ecology and distribution. The correlation of community-based bacterial diversity with the morphology and chemistry of travertine in each facies is a first step toward using carbonate crystal shape and composition as a sensitive indicator of bacterial diversity and activity during carbonate crystal precipitation.

Acknowledgments

This work was supported by research awards from the National Science Foundation Biocomplexity in the Environment Coupled Biogeochemical Cycles Program (EAR 0221743), the National Science Foundation Geosciences Postdoctoral Research Fellowship Program (EAR-0000501), the Petroleum Research Fund of the American Chemical Society Starter Grant Program (34549-G2), and the University of Illinois Urbana-Champaign Critical Research Initiative. Conclusions in this study are those of the authors and do not necessarily reflect those of the funding agencies. Discussions with A. Salyers, C. Woese, N. Goldenfeld, J. Veysey, and H. Garcia throughout the project were essential to improving all aspects of the data collection and interpretation. Thorough reviews provided by B. Chatterton, C. Blank, and J. Thompson served to significantly improve the manuscript.

References

Allen, E.T., and Day, A.L. 1935. Hot Springs of the Yellowstone National Park. Carnegie Institution of Washington, Publication 466.

Altschul, S.F., Gish, W., Miller, W., Meyers, E.W., and Lipman, D.J. 1990. Basic local allignment search tool. Journal of Molecular Biology, **59**: 143–169.

Bargar, K.E. 1978. Geology and thermal history of Mammoth Hot Springs, Yellowstone National Park, Wyoming. United States Geological Survey Bulletin, 1444, 54 p.

Beveridge, T. 1988. Role of cellular design in bacterial metal accumulation and mineralization. Annual Review of Microbiology, **43**: 147–171.

Blank, C.E., Cady, S.L., and Pace, N.R. 2002. Microbial composition of near-boiling silica-depositing thermal springs throughout Yellowstone National Park. Applied and Environmental Microbiology, **68**: 5123–5135.

Blatt, H., Middleton, G.V., and Murray, R.C. 1980. Origin of sedimentary rocks. Prentice-Hall, Englewood Cliffs, N.J.

Boggs, S.J. 2002. Principles of sedimentology and stratigraphy. 3rd ed. Prentice Hall, Upper Saddle River, N.J.

Bonheyo, G.T., Fouke, B.W., Sanzebacher, B., and Salyers, A.A. 2000. By land, sea, or air? microbial transport at the Mammoth Hot Springs complex. GSA Abstracts with Programs, **7(**. 7): A-492.

Brock, T.D., Madigan, M.T., Martinko, J.M., and Parker, J. 2001. Biology of microorganisms. Prentice Hall, Upper Saddle River, N.J.

Farmer, J.D. 2000. Hydrothermal systems: doorways to early biosphere evolution. GSA Today, **10**: 1–8.

Farmer, J.D., and Des Marais, D.J. 1994. Biological versus inorganic processes in stromatolite morphogenesis: observations from mineralizing sedimentary systems. *In* Microbial mats: structure, development, and environmental significance. *Edited by* L.J. Stal and P. Caumette. NATO ASI Series in Ecological Sciences. Springer-Verlag, Berlin and Heidelberg, Germany, pp. 61–68.

Ferris, M.J., Muyzer, G., and Ward, D.M. 1996. Denaturing gradient gel electrophoresis profiles of 16S rRNA-defined populations inhabiting a hot spring microbial mat community. Applied and Environmental Microbiology, **62**: 340–346.

Flügel, E. 1982. Microfacies analysis of limestones. Springer-Verlag, Berlin, Germany.

Ford, T.D., and Pedley, H.M. 1996. A review of tufa and travertine deposits of the world. Earth-Science Reviews, **41**: 117–175.

Fouke, B.W. 2001. Depositional facies and aqueous-solid geochemistry of travertine-depositing hot springs (Angel Terrace, Mammoth Hot Springs, Yellowstone National Park, USA). Journal of Sedimentary Research, **71**: 497–500.

Fouke, B.W., Farmer, J.D., Des Marais, D.J., Pratt, L., Sturchio, N.C., Burns, P.C., and Discipulo, M.K. 2000. Depositional facies and aqueous-solid geochemistry of travertine-depositing hot springs (Angel Terrace, Mammoth Hot Springs, Yellowstone National Park, USA). Journal of Sedimentary Research, **70**: 265–285.

Friedman, I. 1970. Some investigations of the deposition of travertine from hot springs: I. The isotope chemistry of a travertine-depositing spring. Geochimica et Cosmochimica Acta, **34**: 1303–1315.

Goebel, B.M., and Stackebrandt, E. 1994. Cultural and phylogenetic analysis of mixed microbial populations found in natural and commercial bioleaching environments. Applied and Environmental Microbiology, **60**: 1614–21.

Hahn, M.W., Moore, E.R.B., and Hofle, M.G. 1999. Bacterial filament formation, a defense mechanism against flagellate grazing, is growth rate controlled in bacteria of different phyla. Applied and Environmental Microbiology, **65**: 25–35.

Hillis, D.M., Moritz, C., and Mable, B.K. 1996. Molecular systematics. Sinauer Associates, Sunderland, Mass.

Huber, J.A., Butterfield, D.A., and Baross, J.A. 2002. Temporal changes in archael diversity and chemistry in a mid-ocean ridge seafloor habitat. Applied and Environmental Microbiology, **68**: 1585–1594.

Hugenholtz, P., Pitulle, C., Hershberger, K.L., and Pace, N.R. 1998*a*. Novel division level diversity in a Yellowstone hot spring. Journal of Bacteriology, **180**: 366–376.

Hugenholtz, P., Pitulle, C., Hershberger, K.L., and Pace, N.R. 1998*b*. Novel division level bacterial diversity in a Yellowstone hot spring. Journal of Bacteriology, **180**: 366–376.

Hughes, J.B., Hellman, J.J., Ricketts, T.H., and Bohannon, B.J.M. 2001. Mini-Review—Counting the Uncountable: Statistical approaches to estimating microbial diversity. Applied and Environmental Microbiology, **67**: 4399–4406.

Hurst, C.J., Crawford, R.L., Knudsen, G.R., McInernery, M.J., and Stetzenbach, L.D. 2002. Manual of environmental microbiology. ASM Press, Washington, D.C.

Maidik, B.L., Olsen, G.J., Larsen, N., Overbeek, R., Mccaughey, M.J., and Woese, C.R. 1997. The RDP (Ribosomal Database Project). Nucleic Acids, **25**: 109–110.

Martin, A.P. 2002. Phylogenetic approaches for describing and comparing the diversity of microbial communities: Applied and Environmental Microbiology, **68**:. 3673–3682.

Messing, J. 1983. New M13 cloning vectors. Methods in Enzymology, **101**: 20–78.

Newman, D.K., Beveridge, T.J., and Morell, F.M.M. 1997. Precipitation of arsenic trisulfide by Desulfotomacuum auripigmentum. Applied and Environmental Microbiology, **63**: 2022–2028.

Pace, N.R. 1997. A molecular view of microbial diversity and the biosphere. Science (Washington, D.C.), **276**: 734–740.

Pentecost, A. 1990. The formation of travertine shrubs: Mammoth Hot Springs, Wyoming. Geological Magazine, **127**: 159–168.

Pentecost, A., and Viles, H.A. 1994. A review and reassessment of travertine classification. Geographie Physique et Quaternaire, **48**: 305–314.

Reading, H.G. 1996. Sedimentary environments: processes, facies and stratigraphy. Blackwell Science, London, England.

Reysenbach, A.L., Setzinger, S., Kirshtein, J., and Mclaughlin, E. 1999. Molecular constraints on a high-temperature evolution of early life. Biological Bulletin, **196**: 367–372.

Reysenbach, A.L., Ehringer, M., and Hershberger, K.L. 2000*a*. Microbial diversity at 83 °C in Calcite Springs, Yellowstone National Park: another environment where Aquificales and "Korarchaeota" coexist. Extremophiles, **4**: 61–67.

Reysenbach, A.L., Banta, A., Boone, D., Cary, S., and Luther, G. 2000*b*. Microbial essentials at hydrothermal vents. Nature (London), **404**: 835.

Sambrook, J., Fritsch, E.F., and Maniatis, T. 1989. Molecular cloning. A laboratory manual, Cold Spring Harbor Laboratory Press.

Skirnisdottir, S., Hreggvidsson, G.O., Hjorleifsdottir, S., Marteinsson, V.T., Petursdottir, S.K., Holst, O., and Kristjansson, J.K. 2000. Influence of sulfide and temperature on species composition and community structure of hot spring microbial mats. Applied and Environmental Microbiology, **66**: 2835–2841.

Stahl, D.A., Lane, D.J., Olsen, G.J., and Pace, N.R. 1985. Characterization of a Yellowstone hot spring microbial community. Applied Environmental Microbiology, **49**: 1379–1384.

Studier, W.F., and Dunn, J.J. 1983. Complete nucleotide sequence of bacteriophage T7 DNA and the location of T7 genetic elements. Journal of Molecular Biology, **166**: 477–535.

Suzuki, M., Nakagawa, Y., Harayama, S., and Yamamoto, S. 2001. Phylogenetic analysis and taxonoimic study of marine Cytophaga-like bacteria. Journal of Systematic Evolutionary Microbiology, **5**: 1639–1652.

Takacs, C.D., Ehringer, M., Favre, R., Cermola, M., Eggertson, G., Palsdottir, A., and Reysenbach, A.L. 2002. Phylogenetic chracaterization of the blue green filamentous bacterial community from an Icelandic geothermal spring. FEMS Microbiology and Ecology, **35**: 123–128.

Vasconcelos, C., and Mckenzie, J.A. 1997. Microbial Meditation of Modern Dolomite Precipitation and Diagenesis Under Anoxic Conditions (Lagoa Vermelha, Rio De Janero, Brazil). Journal of Sedimentary Research, **67**: 378–390.

Vieira, J., and Messing, J. 1982. The pUC plasmids, an M13mp7-derived system for insertion mutagenesis and sequencing with synthetic universal primers. Gene (Amsterdam), **19**: 259–268.

Walker, R.G., and James, N.P. 1992. Facies Models: response to sea level change. GeoText 1, Geological Association of Canada.

Ward, D.M., Ferris, M.J., Nold, S.C., and Bateson, M.M. 1998. A natural view of microbial biodiversity within hot spring cyanobacterial mat communities. Microbiology and Moelcular Biology Reviews, **62**: 1353–1370.

Whitman, W.B. 1998. Prokaryotes: the unseen majority. Proceedings of the National Academy of Science, **95**: 6578–6583.

Wilmotte, A., Van der Auwera, G., and DeWachter, R. 1993. Structure of the 16S ribosomal RNA of the thermophilic cyanobacterium Chlorogloeopsis HTF (Mastigocladus laminosus HTF) strain PCC7518, and phylogenetic analysis. FEBS Letters, **317**: 96–100.

Wilson, J.L. 1975. Carbonate facies in geologic history. Springer-Verlag, New York.

Woese, C.R. 1987. Bacterial evolution. Microbiology Reviews, **51**: 221–271.

Zak, E., Norling, B., Maitra, R., Huang, F., Anderson, B., and Pakrasi, H. 2001. The initial steps of biogenesis of cyanobacterial photosystems occur in plasma membranes. Proceeding of the National Academies of Science, **98**: 13 443 – 13 448.